DOI: 10.1007/s11099-016-0648-1 PHOTOSYNTHETICA 54 (4): 581-588, 2016

Relationship of photosynthetic efficiency and seed-setting rate in two contrasting rice cultivars under chilling stress

L.-Z. WANG, L.-M. WANG, H.-T. XIANG, Y. LUO, R. LI, Z.-J. LI, C.-Y. WANG, and Y. MENG+

Crop Tillage and Cultivation Institute, Heilongjiang Academy of Agricultural Sciences, Harbin Heilongjiang 150086, China

Abstract

Low temperature during the vegetative stage affects rice (*Oryza sativa* L.) seed-setting rate in Heilongjiang province at Northeast China. However, little is known about changes of the photosynthetic rate and physiological response in contrasting rice cultivars during chilling periods. In this study, two rice cultivars with different chilling tolerance were treated with 15°C from June 27 to July 7. The chilling-susceptive cultivar, Longjing11 (LJ11), showed a significant decrease in a ripening rate and seed-setting rate after being treated for four days, whilst chilling-tolerant cultivar, Kongyu131 (KY131), was only slightly affected after 4-d treatment. The photosynthetic activities, chlorophyll contents, and antioxidative enzyme activities in LJ11 decreased significantly along with the chilling treatment. The decrease in β-carotene contents might play a role as it could cause direct photooxidation of chlorophylls and lead to the inhibition of the photosynthetic apparatus. In the meantime, no significant damage was found in leaves of KY131 from June 27 to July 11. In conclusion, the chilling-tolerance mechanism of rice is tightly related to the photosynthetic rate, metabolism of reactive oxygen species, and scavenging system in the vegetative stage.

Additional key words: abscisic acid; chlorophyll fluorescence; malondialdehyde; peroxidase; proline; superoxide dismutase.

Introduction

Chilling stress is a major factor limiting rice production (Zhao *et al*. 2013a). It is because cultivated rice originates in tropical areas. Chilling affects rice during germination, seedling development, heading, seed formation, and finally also the rice yield. In order to explore inner mechanisms of chilling tolerance and sensitivity in rice cultivars, physiological and molecular techniques were used. For instance, 106 primary metabolites, amino acids (AAs), and related genes, which were recognized and were chilling responsive, contributed greatly to the chilling tolerance of rice variety Lijiangxintuanhegu (LTH) comparing to chilling-sensitive rice variety, IR29 (Zhao *et al*. 2013a). At the transcriptome level, CBF and MYBS3 regulons were involved in the chilling-stress tolerance (Zhang *et al*. 2012b). Regulation clusters responding directly to oxidative signals were related to bZIP factors, ERF factors, and R2R3-MYB factors in chilling-tolerant rice (Yun *et al*. 2010). A subgroup of aquaporins, *OsPIP1;1*, *OsPIP2;1*, and *OsPIP2;7* improved chilling tolerance of the plants by affecting their water balance under chilling stress (Yu *et al*. 2006, Matsumoto *et al*. 2009). Heat shock-mediated *APX* gene was also related to chilling injury in rice seedlings (Sato *et al*. 2001). From the physiological point of view, chilling stress was also related to photooxidation (Wise and Naylor 1987), oxidative stress (Prasad *et al*. 1994), water stress (Takahashi *et al*. 1994), and proton pumping (Kasamo *et al*. 2000). Deficiency of phytochrome B alleviates chilling-induced photoinhibition in rice (Yang *et al*. 2013). The main interaction between chilling tolerance and oxidative burst concerned function of the chloroplasts, especially genes of sucrose metabolism (Jeong *et al*. 2002, Guo *et al*. 2006).

Received 30 October 2015, *accepted* 13 May 2016, *published as online-first* 5 August 2016.
+Corresponding author; phone: +86-0451-86688473, fax: +86-0451-86668732, e-mail: mengying1209@126.com
Abbreviations: ABA – abscisic acid; Chl – chlorophyll; ETR – electron transport rate; F_0 – minimal fluorescence level in dark-adapted leaves; F_0' – minimal fluorescence level in light-adapted leaves; F_m – maximal fluorescence level in dark-adapted leaves; F_m' – maximal fluorescence level in light-adapted leaves; F_v – variable fluorescence level in dark-adapted leaves; F_v' – variable fluorescence level in light-adapted leaves; F_v/F_m – maximal efficiency of PSII photochemistry; F_v'/F_m' – efficiency of excitation energy capture by open PSII reaction centers; KY131 – chilling tolerant cv.; LJ11 – chilling-susceptible cv.; MDA – malondialdehyde; NBT – nitroblue tetrazolium; NPQ – nonphotochemical quenching; POD – peroxidase; q_P – photochemical quenching coefficient; SOD – superoxide dismutase; β-Car – β-carotene; Φ_{PSII} – actual photochemical efficiency of PSII.
Acknowledgements: This work was supported by National Science and Technology Support Project (2012BAD20B0304).

The growth of rice plants is divided into three phases, vegetative (germination to panicle initiation), reproductive (panicle initiation to flowering), and ripening (flowering to mature grain). Heilongjiang province is a main production area of rice cultivars. However, the rice growing season is affected usually by chilling stress from June to July. Chilling stress was associated with soil, irrigation water (Suzuki *et al*. 2014), and air temperature. This is crucial time for panicle initiation and seed setting. However, little is known about the chilling mechanism in rice at the vegetative and seed-setting stage in Heilongjiang Province, China. In order to select a chilling-tolerant cultivar for future breeding programs, two rice cultivars contrasting in chilling tolerance were used for our experiments. Changes in their photosynthetic capacities and antioxidative enzyme activities were assayed for elucidation of chilling-tolerance mechanism in rice.

Materials and methods

Plant material: Rice chilling-tolerant cultivar, Kongyu131 (KY131), and chilling-sensitive cultivar, Longjing11 (LJ11), were used for chilling experimets. Seeds germinated on 28 April were used in 2012–2014. Seedlings with four leaves were planted in black soils of experimental farm in Harbin City, Heilongjiang province (45°75'27"N, 126°63'19"E). During the growing season, the average temperature was about 25–32°C, precipitation was about 36–170 mm, and humidity was around 60%. Chilling treatments were peformed in a control greenhouse at 15°C, the whole seedlings were treated for 4 d from 23 June, 25 June, 27 June, 29 June, 1 July, 3 July, 5 July, 7 July, 9 July, and 11 July, respectively. Seedlings were planted in field for final measurements of the seed-setting rate (Zhao *et al.* 2006).

Chlorophyll (Chl) was extracted with 80% ice cold acetone from 0.1 g of leaf samples. The extract was measured spectrophotometrically at 475, 645, and 663 nm with *GE Ultrospec™ 2100 pro UV/Visible* spectrophotometer (*GE Healthcare*, USA) according to Lichtenthaler (1987).

Modulated Chl fluorescence was measured in attached leaves at midday with a *PAM-2500* portable fluorometer (*Walz*, Germany) connected to a computer with data acquisition software *PAMwin3*. The minimal fluorescence level (F_0) in dark-adapted state was determined by the measuring modulated light, which was sufficiently low [<0.1 μmol(photon) m^{-2} s^{-1}] not to induce any significant variable fluorescence. In order to determine the minimal fluorescence level during illumination (F_0'), a black cloth was rapidly placed around the leaf and the leaf-clip holder in the presence of far-red light [7 μmol(photon) m^{-2} s^{-1}] in order to oxidize fully the PSII centres. Upon darkening of the leaf for 30 min, fluorescence dropped to the F_0' level and immediately rose again within several seconds. The maximal fluorescence in the dark-adapted state (F_m) and the maximal fluorescence during natural illumination (F_m') were measured by a 0.8-s saturating pulse at 8,000 μmol(photon) m^{-2} s^{-1}. F_m was measured after 30 min of dark adaptation. F_m' and F_s were measured at PPFD of approximately 1,400 and 200 μmol m^{-2} s^{-1}, respectively, by a 0.8-s saturating pulse. Other parameters were calculated based on measured parameters above (Demmig-Adams *et al*. 1996).

Abscisic acid (ABA): 0.5–1.0 g of fresh leaves was homogenized with 2 ml of 80% ice cold methanol, containing 1 mmol L^{-1} 2,6-di-tert-butyl-4-methylphenol on ice. After a full extraction for 4 h at 4°C, the supernatant was obtained by centrifugation at 1,000 × *g*, at 4°C, for 15 min and then was passed through C-18 solid phase extract column. Samples were air-dried with liquid N and resuspended by 1.5 ml of phosphate buffered saline buffer with 1:1,000 (v/v) Tween-20 and 1:1,000 (w/v) glutin, pH 7.5. ABA determination was performed with the ELISA method with ABA antigen, antibody, and ABA standard. Secondary antibodies were goat antirabbit IgG coupled with horseradish peroxidase. The optical density was measured by *DNA EXPERT* (*Tecan*, Austria) at 490 nm (Wang and Chen 2011).

Antioxidative enzyme activities: Superoxide dismutase (SOD, EC 1.15.1.1) activity was assayed by monitoring the inhibition of photochemical reduction of nitroblue tetrazolium (NBT) with some modifications. For the total SOD assay, 5 ml of the reaction mixture contained 50 mM HEPES (pH 7.6), 0.1 mM EDTA, 50 mM Na_2CO_3, 13 mM methionine, 0.025% (w/v) Triton X-100, 75 μM NBT, 2 μM riboflavin, and an appropriate aliquot of the enzyme extract. The reaction mixtures were illuminated for 15 min at a light intensity of 350 μmol(photon) m^{-2} s^{-1}. One unit of SOD activity was defined as the amount of enzyme required to cause 50% inhibition of the reduction of NBT as monitored at 560 nm. Peroxidase (POD, EC 1.11.1.7) activity was assayed with guaiacol as the hydrogen donor with extinction coefficient of 26.6 mM cm^{-1} at 470 nm. The reaction mixture consisted of 0.25% (v/v) guaiacol and 0.1 M H_2O_2 in 10 mM sodium phosphate buffer, pH 6.0. A series of dilutions of the crude enzyme preparations (0.1 ml) were added to 3 ml of the reaction mixture. Changes in absorbance at 470 nm from 0, 1, 2, and 3 min were recorded, and the activity of peroxidase was expressed as μmol(product) min^{-1} g^{-1}(FM) (Ye *et al*. 1990). Enzyme activities were measured with *GE Ultrospec™ 2100 pro UV/Visible* spectrophotometer (*GE Healthcare*, USA).

Proline and malondialdehyde (MDA): For the proline assay, leaf samples (0.5 g) were homogenized in 10 ml of 3% sulfosalicylic and the homogenate was filtered through

filter paper. Extract (2 ml) was added to 2 ml of glacial acetic acid and 2 ml of acid-ninhydrin and heated in water bath for 30 min. After cooling down, 4 ml of methylbenzene were added with agitation. The absorbance of the red methylbenzene supernatant was recorded at 520 nm with *GE Ultrospec™ 2100 pro UV/Visible* spectrophotometer (*GE Healthcare*, USA). The MDA content was assayed by the thiobarbituric acid method. Leaf samples (0.1 g) were homogenized in 5 ml of 0.05 M phosphate buffer (pH 7.8) at 4°C. The homogenate was centrifuged at 12,000 × *g* for 20 min. Then, 2.5 ml of 20% (w/v) trichloracetic acid (TCA) containing 0.5% (w/v) thiobarbituric acid (TBA) was added to 1.5 ml of the supernatant. The mixture was heated in boiling water for 10 min and then quickly cooled in an ice bath. After the tube was centrifuged at 1,800 × *g* for 10 min, the absorbance of the supernatant was recorded at 532, 600, and 450 nm with *GE Ultrospec™ 2100 pro UV/Visible* spectrophotometer (*GE Healthcare*, USA). MDA concentrations were calculated by the formula: MDA [μmol L^{-1}] = 6.45 × (A_{532} – A_{600}) – 0.56 × A_{450}.

Statistical analysis: All data were analyzed by *IBM-SPSS* analytical software package *version 21.0* (*IBM Corporation*, USA). One-way analysis of variance (*ANOVA)* and the *Duncan*'s test was used for statistical analysis. The probability level of $P<0.01$ was considered significant. Figures were drawn by *OriginPro2015* software (*OriginLab Corporation*, USA). All of the measurements were performed six times, the means and calculated standard deviations (SD) were reported.

Results

Different treatment days showed a significant difference in the ripening rate and stem seed-setting rate, especially from 29 June to 3 July in the chilling-sensitive cultivar LJ11 (Table 1). The ripening rate was reduced from 80.3% on 23 June to 51.8% on 3 July. The seed-setting rate was reduced from 85.1% on 9 July to 55.0% on 1 July. By contrast, chilling-tolerant KY131 showed a slight decrease of the ripening rate and stem seed-setting rate from 1 to 5 July after the chilling treatment for four days. The ripening rate was more than 80%, and seed-setting rate was more than 73%.

Usually, chilling tolerance was related to the early response and photosynthesis of rice, therefore we measured a Chl content of the chilling-treated leaves after four days of the treatment.

The leaves treated for 4 d showed a great change in their Chl contents. Both Chl *a* and Chl *b* contents decreased significantly from 29 June to 3 July (Fig. 1). It suggested that in this period the leaf development was affected seriously by chilling treatment. The retardation of leaves directly affected a subsequent seed formation rate. The reduction of Chl *a* was faster than that of Chl *b* from 1–5 July and resulted in the decrease of the Chl *a*/*b* ratio. β-carotene (β-Car) contents decreased significantly in the leaves treated on 29 June and 3 July; this suggested that serious photooxidation occured after the chilling treatment. By contrast, in the chilling-tolerant KY131 leaves, the Chl contents did not change significantly (Fig. 2).

The maximal efficiency of PSII photochemistry (F_v/F_m) decreased significantly in the leaves treated on 27 June and 1 July (Fig. 3). The electron transport rate (ETR), photochemical quenching (q_P), and the actual photochemical efficiency of PSII (Φ_{PSII}) showed more dramatic decrease in the leaves treated on 27 June and 1 July. In contrast, the nonphotochemical quenching (NPQ) increased nearly by 50% during this period. The photosynthetic rate of KY131 did not show any significant change at the same time (Fig. 4).

SOD and POD enzyme activity decreased significantly from 27 June and 1 July in treated leaves. Other stress-related indices, such as the proline, MDA, and ABA contents increased significantly (Fig. 5).

By contrast, in the chilling-tolerant KY131 plants, the stress-related indices did not change significantly (Fig. 6). The enzyme activities and stress-related indices coincided with the reduction of ripening rate and seed-setting rate in both rice cultivar.

Table 1. Effects of chilling treatment on the seed-setting rate and ripening rate of cultivars LJ11 and KY131. Differernt *uppercase letters* mean significant level ($P<0.01$) by *ANOVA* and *Duncan*'s test.

Treatment day	LJ11 Ripening rate [%]	LJ11 Seed-setting rate [%]	KY131 Ripening rate [%]	KY131 Seed-setting rate [%]
23 June	80.27 ± 3.10^{A}	77.02 ± 9.59^{AB}	88.13 ± 1.57^{AB}	84.16 ± 6.54
25 June	72.57 ± 9.04^{ABC}	79.08 ± 4.00^{AB}	87.51 ± 3.14^{AB}	83.19 ± 6.18
27 June	69.51 ± 5.51^{ABCD}	66.84 ± 16.84^{AB}	89.05 ± 1.41^{AB}	83.02 ± 7.17
29 June	59.29 ± 9.88^{BCD}	67.08 ± 14.79^{AB}	89.31 ± 2.68^{A}	86.81 ± 5.03
1 July	56.16 ± 6.49^{CD}	54.95 ± 10.30^{B}	84.52 ± 3.66^{ABCD}	77.21 ± 8.97
3 July	51.79 ± 5.17^{D}	66.34 ± 7.77^{AB}	81.19 ± 3.37^{CD}	74.89 ± 7.73
5 July	62.48 ± 9.31^{ABCD}	78.52 ± 7.04^{AB}	80.84 ± 2.01^{D}	84.51 ± 6.09
7 July	75.63 ± 11.93^{ABC}	85.72 ± 5.48^{A}	82.75 ± 3.28^{ABCD}	82.64 ± 4.70
9 July	72.89 ± 17.32^{ABC}	85.08 ± 9.91^{A}	87.45 ± 2.87^{ABC}	86.09 ± 5.38
11 July	79.75 ± 8.87^{AB}	74.34 ± 17.24^{AB}	84.16 ± 3.51^{ABCD}	73.54 ± 6.86

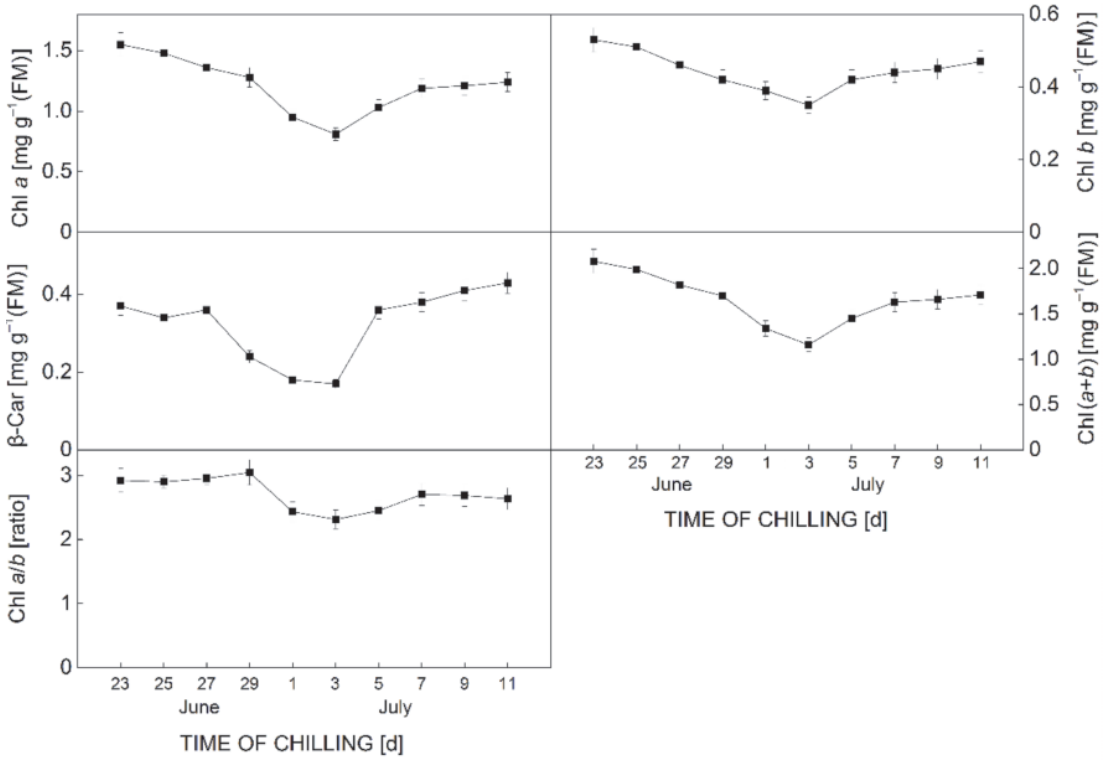

Fig. 1. Changes of chlorophyll (Chl) and β-carotene (β-Car) contents of chilling-treated seedlings of chilling-susceptible rice cultivar LJ11. FM – fresh mass.

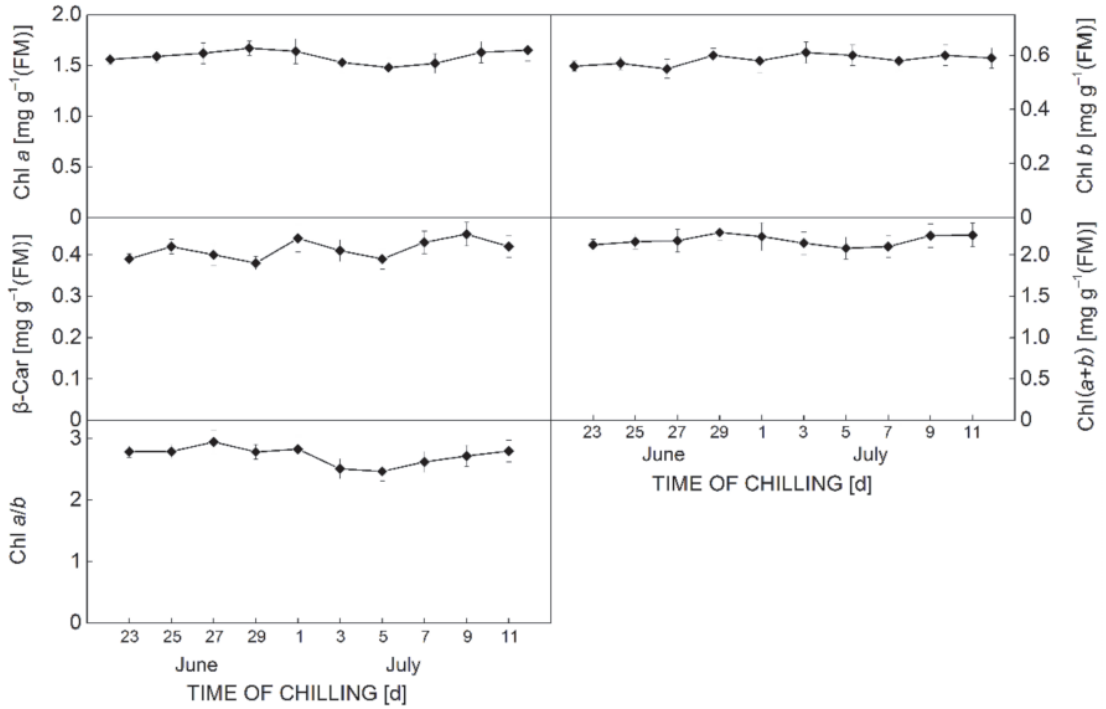

Fig. 2. Changes of chlorophyll (Chl) and β-carotene (β-Car) contents of chilling-treated seddlings of chilling-tolerant rice cultivar KY131. FM – fresh mass.

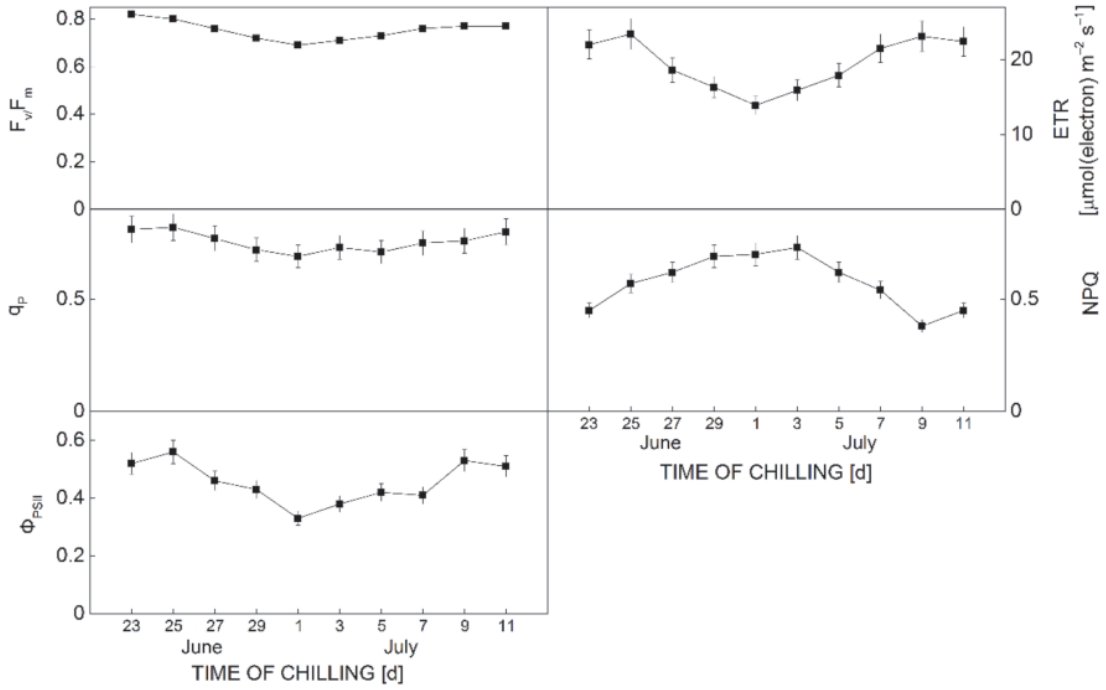

Fig. 3. Changes of chlorophyll *a* fluorescence parameters of chilling-treated seedlings of chilling-susceptible rice cultivar LJ11. ETR – electron transport rate; F_v/F_m – maximal efficiency of PSII photochemistry; NPQ – nonphotochemical quenching; q_P – photochemical quenching coefficient; Φ_{PSII} – actual photochemical efficiency of PSII.

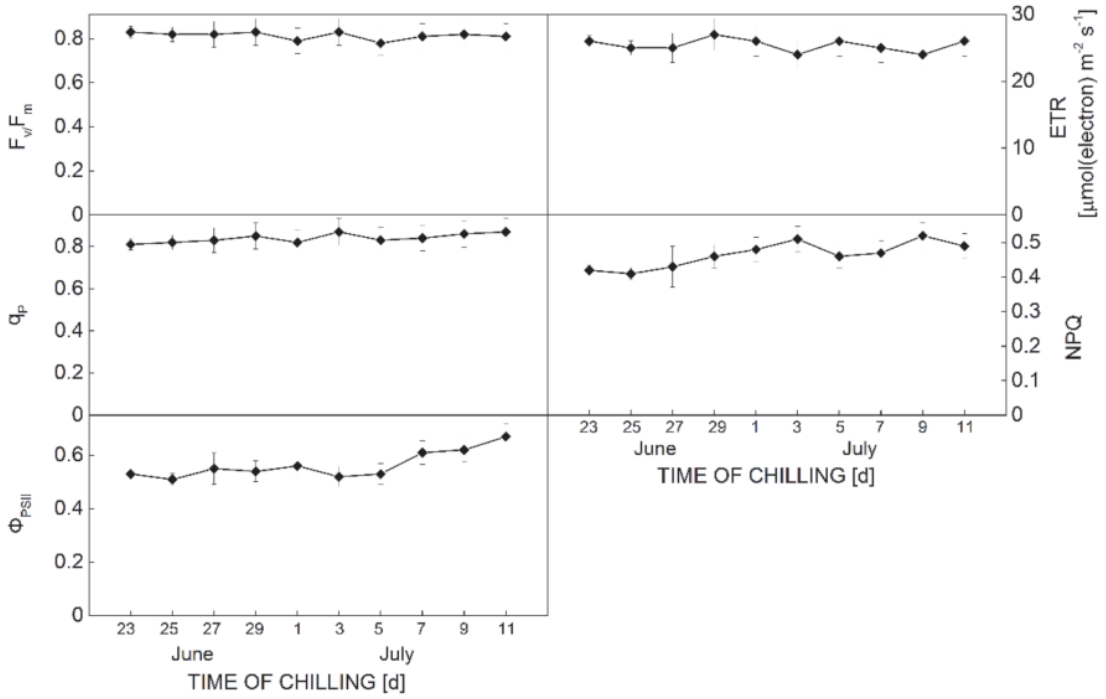

Fig. 4. Changes of chlorophyll *a* fluorescence parameters of chilling-treated seedlings of chilling-tolerant rice cultivar KY131. ETR – electron transport rate; F_v/F_m – maximal efficiency of PSII photochemistry; NPQ – nonphotochemical quenching; q_P – photochemical quenching coefficient; Φ_{PSII} – actual photochemical efficiency of PSII.

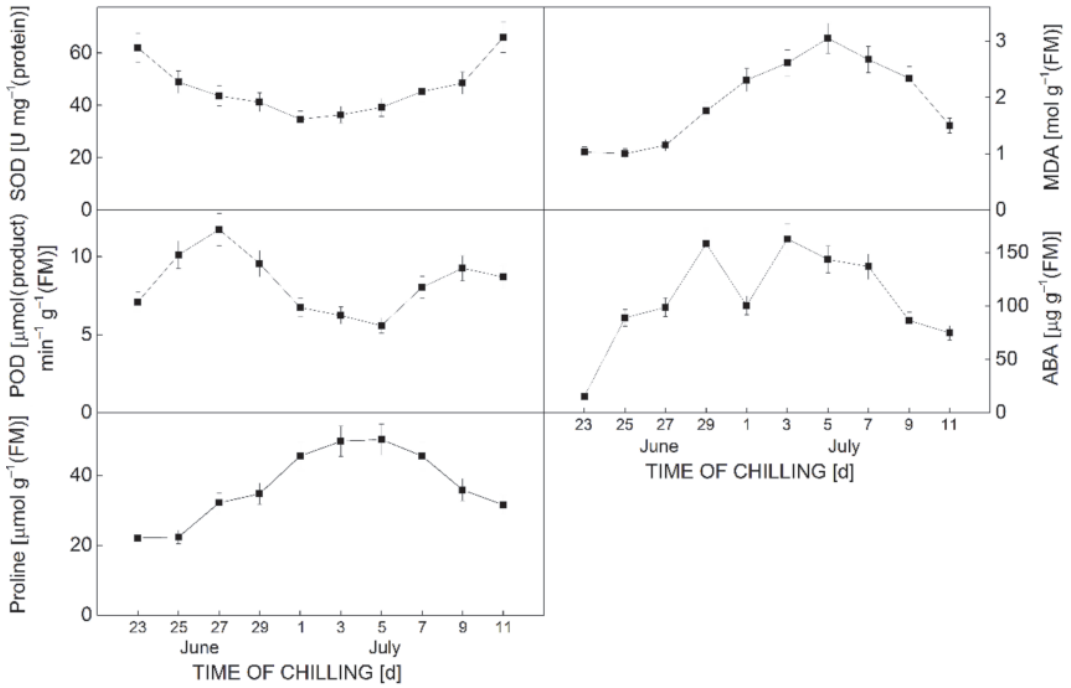

Fig. 5. Changes of physiological parameters of chilling-treated seedlings of chilling-susceptible rice cultivar LJ11. ABA – abscisic acid; MDA – malondialdehyde; POD – peroxidase; SOD – superoxide dismutase.

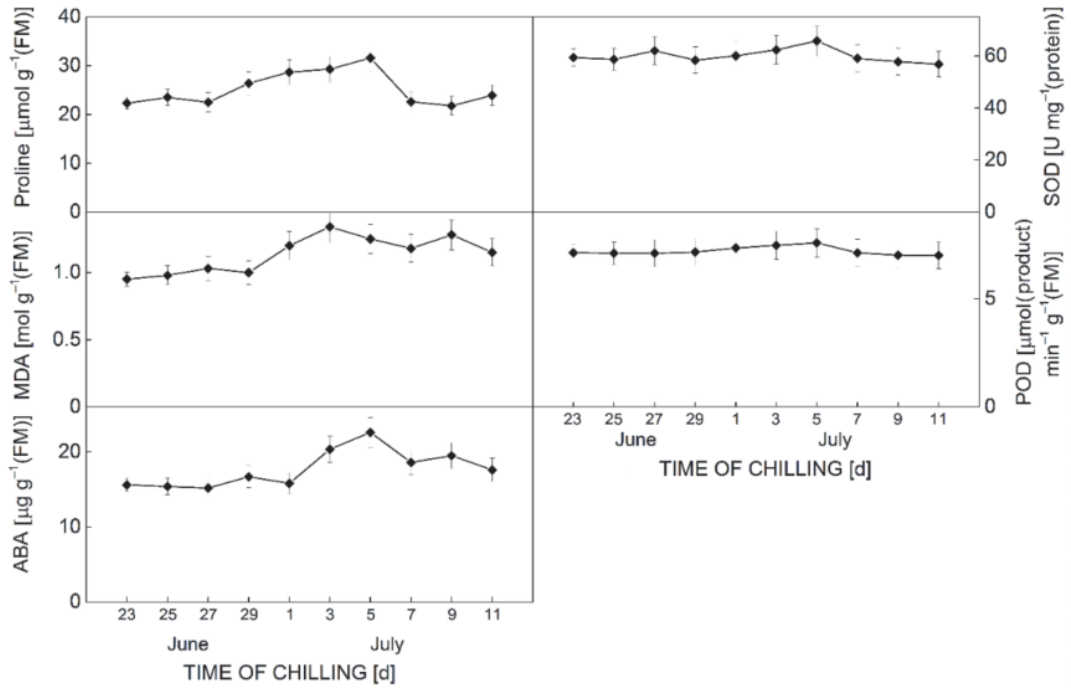

Fig. 6. Changes of physiological parameters of chilling-treated seedlings of chilling-tolerant rice cultivar KY131. ABA – abscisic acid; MDA – malondialdehyde; POD – peroxidase; SOD – superoxide dismutase.

Discussion

Chilling is considered being related to reactive oxygen species (ROS), enzyme activities (del Río *et al*. 1977), and photosystem functioning (Smillie and Nott 1979). The damage of leaves during chilling stress leads to male sterility and to a final yield loss (Noctor 2015). This is due to ATP synthesis reduction (Kasamo *et al.* 2000) and

contents of phosphatidylglycerol (PG) of thylakoid membrane lipids (Zhu *et al.* 2008). Although no significant change in leaf color was observed, chloroplast structure changes in chilled leaves and swelling or disintergration of thylakoid membranes occur (Kratsch and Wise 2000).

In this study, we confirmed that the chilling stress from 29 June to 5 July occurred during the most sensitive period for the LJ11 cultivar of rice. Although treated only for four days, the damage seemed to be irreversible and led to a final loss of 30–40% ripening rate and seed-settting rate (Table 1).

The straight degradation of Chl *a* and Chl *b* is an indicator of plant damage, which is associated with an increase of chlorophyllase activity in Chl-catabolic pathway (Hörtensteiner 2006). The faster degradation of Chl *a* than that of Chl *b* resulted in the decrease of the Chl *a*/*b* ratio (Fig. 1). β-Car can usually quench ROS at the early stage of a damage (Apel and Hirt 2004). On the contrary, the decrease in the Car contents can directly cause photo-oxidation of Chls and may lead to the partial destruction of the photosynthetic apparatus. The chiling treatment did not only affect the contents of Chl, but it reduced the absorption efficiency of Chl and also reduced the contents of Car. Besides, a straight decrease of F_v/F_m, ETR, and q_P in the chilling-treated leaves suggested a potential damaging effect of light on PSII, which could be observed also in changes of chloroplast structure (Kratsch and Wise 2000). The increase of NPQ indicated that after chilling-induced decrease in PSII functioning; the light energy absorbed by chloroplasts could not be transferred to PSI, but dissipated as heat through nonphotochemical quenching (Roháček and Barták 1999, Roháček 2002).

The breakdown of photosynthetic electron transport chain also increased ROS contents as shown in other plants (Hodges *et al.* 1997, Michaeli *et al.* 1999, Lee and Lee 2000). SOD is the first enzyme controlling oxidative stress (Alscher *et al.* 2002). Our findings revealed that the chilling caused the increase of defense-responsive enzyme activities in order to cope with the damage of lipid membrane and protein in plant cell and increased stress indicators, ABA under chilling stress (Zhang *et al.* 2012a, Zhao *et al.* 2013b). The relatively high contents of MDA as well as the enzyme activity of SOD and POD indicated that chilling stress was accompanied by oxidative stress (Fig. 3). The MDA content in plant tissues is considered an index of membrane oxidation (Chia *et al.* 1981). ABA is one of the most important plant hormones regulating stress-responsive processes (Halevy *et al.* 1974, Yang *et al.* 2002, Hung and Kao 2004, Yang *et al.* 2011). The significant increase of MDA and ABA contents, especially in the plants treated from 29 June to 5 July, indicated that LJ11 was affected by chilling stress.

Conclusion: We found that the chilling-tolerant mechanism was tightly related to the photosynthetic rate, ROS metabolism, and ROS scavenging system.

References

Alscher R.G., Erturk N., Heath L.S.: Role of superoxide dismutases (SODs) in controlling oxidative stress in plants. – J. Exp. Bot. **53**: 1331-1341, 2002.

Apel K., Hirt H.: Reactive oxygen species: metabolism, oxidative stress, and signal transduction. – Annu. Rev. Plant Biol. **55**: 373-399, 2004.

Chia L.S., Thompson J.E., Dumbroff E.B.: Simulation of the effects of leaf senescence on membranes by treatment with paraquat. – Plant Physiol. **67**: 415-420, 1981.

del Río L.A., Gómez M., López-Gorgé J.: Catalase and peroxidase activities, chlorophyll and proteins during storage of pea plants of chilling temperatures. – Rev. Esp. Fisiol. **33**: 143-148, 1977.

Guo Z., Ou W., Lu S., Zhong Q.: Differential responses of antioxidative system to chilling and drought in four rice cultivars differing in sensitivity. – Plant Physiol. Bioch. **44**: 828-836, 2006.

Halevy A., Mayak S., Tirosh T. *et al.*: Opposing effects of abscisic acid on senescence of rose flowers. – Plant Cell. Physiol. **15**: 813-821, 1974.

Hodges D.M., Andrews C.J., Johnson D.A., Hamilton R.I.: Antioxidant enzyme responses to chilling stress in differentially sensitive inbred maize lines. – J. Exp. Bot. **48**: 1105-1113, 1997.

Hörtensteiner S.: Chlorophyll degradation during senescence. – Annu. Rev. Plant Biol. **57**: 55-77, 2006.

Hung K.T., Kao C.H.: Hydrogen peroxide is necessary for abscisic acid-induced senescence of rice leaves. – J. Plant Physiol. **161**: 1347-1357, 2004.

Jeong S.W., Choi S.M., Lee D.S. *et al.*: Differential susceptibility of photosynthesis to light-chilling stress in rice (*Oryza sativa* L.) depends on the capacity for photochemical dissipation of light. – Mol. Cells **13**: 419-428, 2002.

Kasamo K., Yamaguchi M., Nakamura Y.: Mechanism of the chilling-induced decrease in proton pumping across the tonoplast of rice cells. – Plant Cell Physiol. **41**: 840-849, 2000.

Kratsch H., Wise R.: The ultrastructure of chilling stress. – Plant Cell Environ. **23**: 337-350, 2000.

Lee D.H., Lee C.B.: Chilling stress-induced changes of antioxidant enzymes in the leaves of cucumber: in gel enzyme activity assays. – Plant Sci. **159**: 75-85, 2000.

Lichtenthaler H.K.: Chlorophylls and carotenoids: Pigments of photosynthetic biomembranes. – Methods Enzymol. **148**: 350-382, 1987.

Matsumoto T., Lian H.L., Su W.A. *et al.*: Role of the aquaporin PIP1 subfamily in the chilling tolerance of rice. – Plant Cell Physiol. **50**: 216-229, 2009.

Michaeli R., Philosoph-Hadas S., Riov J., Meir S.: Chilling-induced leaf abscission of *Ixora coccinea* plants. I. Induction by oxidative stress *via* increased sensitivity to ethylene. – Physiol. Plantarum **107**: 166-173, 1999.

Noctor G.: Keeping a cool head: gene networks underlying chilling-induced male sterility in rice. – Plant Cell Environ. **38**: 1252-1254, 2015.

Prasad T.K., Anderson M.D., Martin B.A., Stewart C.R.: Evidence for chilling-induced oxidative stress in maize seedlings

and a regulatory role for hydrogen peroxide. – Plant Cell **6**: 65-74, 1994.

Roháček K.: Chlorophyll fluorescence parameters: the definitions, photosynthetic meaning, and mutual relationships. – Photosynthetica **40**: 13-29, 2002.

Roháček K., Barták M.: Technique of the modulated chlorophyll fluorescence: basic concepts, useful parameters, and some applications. – Photosynthetica **37**: 339-363, 1999.

Sato Y., Murakami T., Funatsuki H. *et al*.: Heat shock-mediated APX gene expression and protection against chilling injury in rice seedlings. – J. Exp. Bot. **52**: 145-151, 2001.

Smillie R.M., Nott R.: Assay of chilling injury in wild and domestic tomatoes based on photosystem activity of the chilled leaves. – Plant Physiol. **63**: 796-801, 1979.

Suzuki K., Aoki N., Matsumura H. *et al*.: Cooling water before panicle initiation increases chilling-induced male sterility and disables chilling-induced expression of genes encoding OsFKBP65 and heat shock proteins in rice spikelets. – Plant Cell Environ. **38**: 1255-1274, 2014.

Takahashi R., Joshee N., Kitagawa Y.: Induction of chilling resistance by water stress, and cDNA sequence analysis and expression of water stress-regulated genes in rice. – Plant Mol. Biol. **26**: 339-352, 1994.

Wang L.F., Chen Y.Y.: Photosynthetic characterization changes at different senescence stages in an early senescence mutant of rice *Oryza sativa* L. – Photosynthetica **49**: 140-144, 2011.

Wise R.R., Naylor A.W.: Chilling-enhanced photooxidation: the peroxidative destruction of lipids during chilling injury to photosynthesis and ultrastructure. – Plant Physiol. **83**: 272-277, 1987.

Yang J., Zhang J., Wang Z. *et al*.: Abscisic acid and cytokinins in the root exudates and leaves and their relationship to senescence and remobilization of carbon reserves in rice subjected to water stress during grain filling. – Planta **215**: 645-652, 2002.

Yang J.C., Li M., Xie X.Z. *et al*.: Deficiency of phytochrome B alleviates chilling-induced photoinhibition in rice. – Am. J. Bot. **100**: 1860-1870, 2013.

Yang S.D., Seo P.J., Yoon H.K., Park C.M.: The *Arabidopsis* NAC transcription factor VNI2 integrates abscisic acid signals into leaf senescence *via* the COR/RD genes. – Plant Cell **23**: 2155-2168, 2011.

Ye X.S., Pan S.Q., Kuc J.: Activity, isozyme pattern, and cellular localization of peroxidase as related to systemic resistance of tobacco to blue mold (*Peronospora tabacina*) and to tobacco mosaic virus. – Phytopathology **80**: 1295-1299, 1990.

Yu X., Peng Y.H., Zhang M.H. *et al*.: Water relations and an expression analysis of plasma membrane intrinsic proteins in sensitive and tolerant rice during chilling and recovery. – Cell Res. **16**: 599-608, 2006.

Yun K.Y., Park M.R., Mohanty B. *et al*.: Transcriptional regulatory network triggered by oxidative signals configures the early response mechanisms of japonica rice to chilling stress. – BMC Plant Biol. **10**: 16, 2010.

Zhang K., Xia X., Zhang Y., Gan S.S.: An ABA-regulated and Golgi-localized protein phosphatase controls water loss during leaf senescence in *Arabidopsis*. – Plant J. **69**: 667-678, 2012a.

Zhang T., Zhao X., Wang W. *et al*.: Comparative transcriptome profiling of chilling stress responsiveness in two contrasting rice genotypes. – PloS One **7**: e43274, 2012b.

Zhao B.H., Wang P., Zhang H.X. *et al*.: Source-sink and grain-filling characteristics of two-line hybrid rice Yangliangyou 6. – Rice Sci. **13**: 34-42, 2006.

Zhao X.Q., Wang W.S., Zhang F. *et al*.: Temporal profiling of primary metabolites under chilling stress and its association with seedling chilling tolerance of rice (*Oryza sativa* L.). – Rice **6**: 23, 2013a.

Zhao Y., Chan Z., Xing L. *et al*.: The unique mode of action of a divergent member of the ABA-receptor protein family in ABA and stress signaling. – Cell Res. **23**: 1380-1395, 2013b.

Zhu S.Q., Zhao H., Liang J.S. *et al*.: Relationships between phosphatidylglycerol molecular species of thylakoid membrane lipids and sensitivities to chilling-induced photoinhibition in rice. – J. Integr. Plant Biol. **50**: 194-202, 2008.